

Cosmic Messengers: Catch Cosmic Rays with Silicon Photomultipliers

Advanced Lab course
Technical University Munich, Physics Department E15

April 12, 2021

1 Overview

1.1 Purpose of the experiment

The vertical flux of cosmic rays shall be measured. The efficiency of the detector is to be estimated by comparison with the expected rate. The concept of this laboratory course is to allow you to set up the experiment. Therefore, there will be no step-by-step instructions, only the objectives and a description of the available equipment. Please consider how you would approach the experiment. You will decide for yourself how to set up the experiment by selecting the equipment to be used and conducting the measurements you deem necessary. The instructor will help you, but will not run the experiment for you. With this "learning-by-doing principle" you will learn the most, in our opinion, about how to prepare, set up, and run an experiment.

1.2 Cosmic Messengers

Cosmic Messengers are signals from the universe with which one can do astronomy. There are four types of messengers; Electromagnetic, cosmic rays, cosmic neutrinos, gravitational waves.

1.2.1 Electromagnetic signal

Since hundreds of years people observed the night-sky with telescopes to learn more about the universe we live in. Over the years those telescopes became more sensitive, increased the sensitive bands and even left earth. Nowadays telescopes are operated which are sensitive for radio waves (e.g. Arecibo Observatory [1]), microwave, sub-millimeter, infrared, optical, UV light (e.g. VLT [2]) and X-rays. Not only on earth but also in the form of satellites, telescopes are operated (e.g. COBE [3])

1.2.2 Cosmic rays

Cosmic ray particles are ionized nuclei, 90% are protons, 9% alpha particles and 1% heavier nuclei. These particles have energies comparable or higher than their masses. A small amount of cosmic rays have energies up to 10^{20} eV (eleven orders of magnitude larger than the rest mass of a proton). To this date the origin of the cosmic rays is not fully understood. The majority originates from within our galaxy but outside the solar system. The highest energetic cosmic rays however show a circular motion in the magnetic field of our galaxy with radii larger than our galaxy. These are most likely from extragalactical origin (see [4]). The hadronic interaction of the cosmic rays

with the atmospheric nuclei leads to a cascading shower of secondary particles like pions and kaons. The pions and kaons decay to muons. The absence of strong interactions and the long lifetime ($\tau = 2.2 \cdot 10^{-6} s$) makes muons (next to neutrinos) the largest fraction of the secondary particles arriving on the earth's surface (see fig. 1) and can travel even far below.

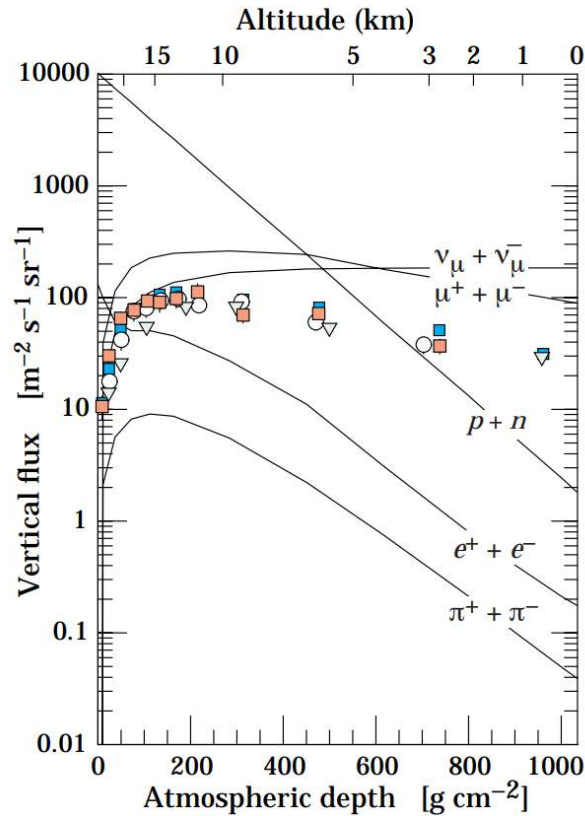


Figure 1: Cosmic vertical flux as a function of altitude and atmospheric depth. (Adapted from [5])

1.2.3 Cosmic Neutrinos

Next to cosmic particles there also exist cosmic neutrinos. Neutrinos react seldom with normal matter and hence make a great messenger for cosmic events near (e.g. solar neutrinos) and far (e.g. the remnants of supernovae) from us, since they can travel to us without mostly any disturbance. Due to the low interaction, it is also very hard to detect those cosmic messengers. Generally there are two approaches to detect these neutrinos: Large detector volumes in the order of cubic kilometers (e.g. represented at TUM:

IceCube[6] and P-ONE[7]) to increase the probability for an interaction of the neutrino with the detector. The other approach is to reduce the background of the detector so far that over a long measurement period no background events are present, and hence a few neutrino interactions are enough for a physical result. This is usually achieved by setting up the experiment far below the earth (muonic background), using ultra radipure materials to avoid background from radio active decays and deploying very sensible detector systems and analysis methods to not miss a single event. At TUM the following experiments researching cosmic messengers with such low background techniques: Borexino [8], CRESST [9] and LEGEND [10].

1.2.4 Gravitational waves

Gravitational waves, very small disturbances of spacetime are generated by accelerated masses (e.g. black holes, spinning neutron stars, supernovae). Such disturbances can be observed with very sensitive laser interferometer (e.g. LIGO [11]) and can provide inside into the heaviest objects and their behavior in our universe. Gravitational waves are the newest members of the cosmic messengers. The first gravitational wave was observed by LIGO in the summer of 2015. It originates from the merger of two black holes. For this observation the Nobel prize of 2017 was awarded to Rainer Weiss and Kip S. Thorne, together with Barry C. Barish [12].

1.3 Silicon Photomultipliers

Silicon photomultipliers (SiPM) are solid-state detectors capable of detecting extremely weak light. A SiPM consists of thousands of so-called micropixels that allow measurement of a wide range of photons while maintaining single-photon resolution (see fig. 2). Each micropixel is essentially a single-photon avalanche diode (SPAD). When a photon is absorbed in such a SPAD (see photoelectric effect), an electron/hole pair is created. The strong electric field in a SPAD accelerates the charge carrier in such a way that impact ionization of secondary charge carriers occurs; an avalanche of charge carriers is triggered, resulting in a measurable charge output. To stop these avalanches, a so-called quenching resistor is connected in parallel to each SPAD. The three most important parameters of a SiPM are:

- Breakdown voltage: The minimal voltage which has to be applied to the SiPM to produce a charge carrier avalanche.
- Dark count rate (DCR): The dark count rate are events generated by the SiPM in the absence of light (e.g. due to thermal effects). This

noise signal is strongly temperature dependent. As a rule of thumb; every 10K reduction in ambient temperature reduces the DCR by a factor of 2.

- Gain: The gain describes the number of charge carriers generated per initial photon and is proportional to the applied overvoltage (= bias voltage - breakdown voltage). As a rule of thumb, the SiPM should be operated with a few volts overvoltage. A too high overvoltage amplifies the noise (e.g. DCR) more than the light signal.

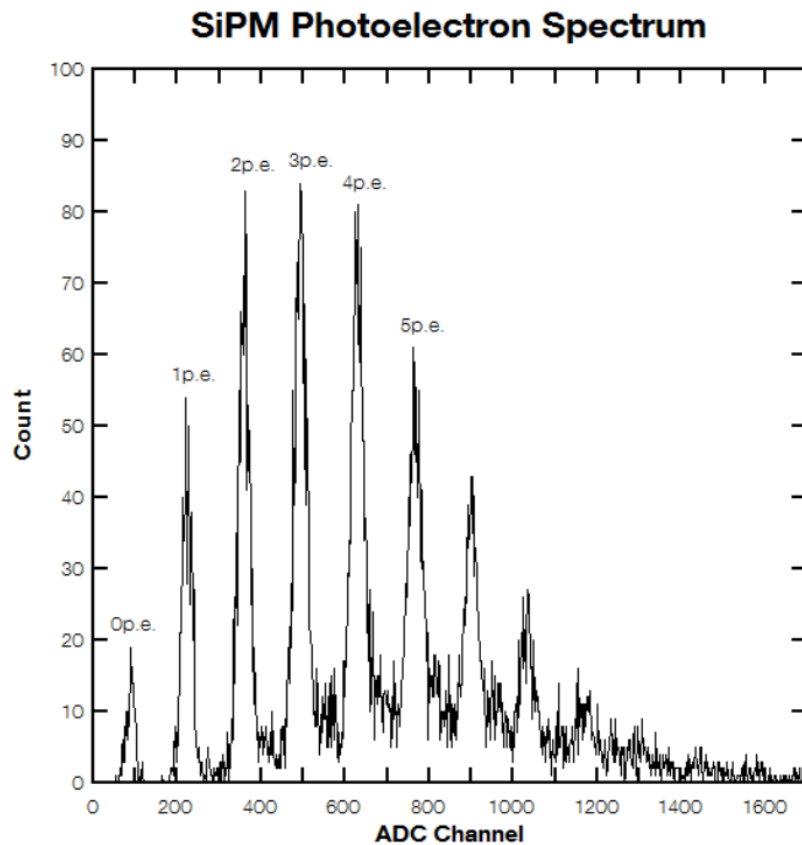


Figure 2: Typical photoelectron spectrum of a SiPM with distinct photoelectron (p.e.) peaks. A photoelectron refers to the primary electron produced from the incident photon. Having several p.e. peaks originates from several micropixels triggering simultaneously (Adapted from [13])

2 Available devices

All of the following devices are available to you, not all of them are of use for the task at hand.

2.1 Power Supply and Amplification Unit

This device combines two components, a power supply and an amplification unit for each of its two channels (see fig. 3). The power supply can provide bias voltages up to 100V with a maximum current of 100 μ A. The integrated temperature controller ensures a stable voltage level even when the temperature of the SiPM changes.

The amplification unit is a wideband amplifier. This means that it has precise amplification over a wide frequency range. The available amplifier has a bandwidth (-3dB) of 100 kHz to 500 MHz. The gain of an amplifier describes the ratio between the output signal and the input signal and is therefore a quantitative statement about the amount of amplification. The available amplifier has a gain of 0 to 50 dB in steps of 1 dB.

The device also provides a digital output generated by a fast edge discriminator. The purpose of a discriminator is to help you decide when the input is something you are interested in. It does this by emitting a logic pulse when the input signal reaches an adjustable threshold. A leading edge discriminator looks only at the leading edge of the signal and when the signal reaches the threshold, the logic pulse is emitted. The discriminator available for this experiment can have a threshold in the range of -800 mV to 800 mV with a step size of 25 μ V. It is also possible to set the discriminator of the two channels in coincidence, i.e. a signal is only emitted if the discriminators of both channels would see a signal at the same time.



Figure 3: CAEN SPS600 power supply. (Adapted from [14])

2.2 CAEN Desktop Waveform Digitizer

The Desktop Waveform Digitizer (see fig. 4) is a so-called FADC (Flash-Analog-to-Digital Converter), which takes analog input signals and converts them to digitized waveforms, which are a series of digital values (called samples). The samples represent voltage levels at different (equidistant) time positions of the signal. The time delay between samples is the FADC frequency, which can reach up to several GS/s (gigasamples per second).

The available device for this Lab Course has two input channels, i.e. can receive signals from two detectors simultaneously. Both inputs are of the so-called MCX type and have an internal termination of $50\ \Omega$; i.e. matching coaxial cables of $50\ \Omega$ impedance. The maximum sampling frequency is 250 MS/s.

An USB interface allows accessing the device from a PC running a dedicated software (provided by us). The FADC is controlled from the "digitizer" panel, which is part of the LabView GUI (graphical user interface) of the mentioned software.

It is important to correctly set up a trigger, that is the condition, which has to be fulfilled in order to make the FADC record a waveform. One can use the time position, where the voltage level of an input channel exceeds a certain, pre-defined threshold as trigger. This is an example of an internal trigger, since the trigger signal comes from an input line.

The FADC uses a slightly modified internal trigger. There, the height (voltage) difference of the signal at two time points has to exceed a threshold, i.e. the trigger acts on the numerically differentiated signal. Both the time difference ("rise time") as well as the threshold can be set per channel.

It is also possible to let the FADC trigger on coincidences, i.e. on an event where two internal triggers are present for both input lines. The maximum time difference for accepting a coincidence can be set.

External triggers are supplied as logical signals (TTL or NIM)¹ to a special trigger-in input of the FADC.

The gate parameters control the number of samples per waveform.

The baseline parameters control the baseline restoration, i.e. the vertical adjustment in case of a constant voltage offset.

¹Logical signals convey two possible states: logical 1 (high) and 0 (low). There are two common types of logical signals used in nuclear physics, which differ in their definition of the 1 state (the 0 state is always ground potential / no current): TTL signals define 5 V (with minus tolerance) as high state. NIM signals on the other hand define negative currents of roughly $-15\ \text{mA}$ as logical 1, due to the mostly used $50\ \Omega$ terminators this usually leads to a voltage level of about $-700\ \text{mV}$.



Figure 4: CAEN DT5720A Desktop Waveform Digitizer. (Adapted from [14])

2.3 Passive Splitter

As the name suggests, the splitter (see fig. 5) splits up entering signals, which then are emitted equally in both output lines. Since the splitter is completely passive (no input power used), the output amplitudes are reduced (energy conservation). All connections are matched for an impedance of $50\ \Omega$, thus preventing signal reflections given that coaxial cables of an impedance of $50\ \Omega$ are used.



Figure 5: CAEN A315 Passive Splitter (Adapted from [14])

2.4 ultra-fast LED Driver

The ultra-fast LED driver (see fig. 6) provides triggered light pulses of variable intensity and width. The peak of the emitted light spectrum is at 400 nm . The LED driver can be triggered either via the internal pulse generator, or via an external source; the optical signal is output at the back and can be routed to a measurement setup via an optical fiber.

If the internal trigger is used, one can choose the frequency range between LOW (500 Hz to 80 kHz) and HIGH (60 kHz to 5 MHz) and fine-tune it inside this range with the **FREQ** trimmer on the left of the LOW/HIGH switch. **OUT** provides the internal trigger output.

If the external trigger is selected, **IN** provides the external trigger input.

On the back panel one can vary the intensity for every light pulse using the AMPLITUDE turn dial.



Figure 6: CAEN SP5601 ultra-fast LED Driver. (Adapted from [14])

2.5 sensor holder

The holder (see fig. 7) hosts a $1.3 \times 1.3 \text{ mm}^2$ SiPM; moreover, a probe inside the holder senses temperature variations, thus allowing the user to compensate for possible gain instability. The holder is made of a mechanical structure providing a fiber connector and a PCB (printed circuit board) where the SiPM is soldered.



Figure 7: CAEN SP5650C Sensor holder. (Adapted from [14])

2.6 embedded plastic scintillating tile

The tile (see fig. 8), with a sensitive volume of $47 \times 47 \times 10 \text{ mm}^3$, is emitting light upon the interaction with ionizing radiation (e.g. β -radiation). The tile is made of Polystyrene and is directly coupled to a $6 \times 6 \text{ mm}^2$ SiPM and a temperature sensor.

2.7 mini-spectrometer for gamma ray detection

The spectrometer (see fig. 8) consists of a mechanical structure which houses a scintillating crystal, coupled to a SiPM. One can choose from three different crystals:

- CsI: The Cesium-Iodide-Crystal is one of the brightest scintillator crystals known (around 50 photons/keV). The broad emission is situated at 550 nm and has a relatively low density (4.51 g/cm^3). This scintillator is relatively slow with an average decay time of $1\mu\text{s}$.
- LYSO: A Cerium doped Lutetium based scintillation crystal yields around 30 photons/keV. The emission peak is at 420 nm and it has density of 7.1 g/cm^3 . This scintillator is very fast with an average decay time of 36 ns.
- BGO: The Bismuth Germanate Scintillator crystal has a photon yield of around 15 photons/keV. The emission maximum is 480 nm and has a relative high density (7.2 g/cm^3). The decay time of BGO is around 300 ns.

One can see that each of that three crystals has its strong suit.



Figure 8: CAEN SP5606 Mini spectrometer (front) and CAEN SP5608 Embedded plastic scintillating tile (back). (Adapted from [14])

2.8 Gamma absorption tool

The Gamma absorption tool (see fig. 9) allows to perform gamma attenuation measurements. It is a modular tool and its design allows an easy connection to the mini spectrometer (sec. 2.7). The tool is composed of two different absorber materials: aluminum and PMMA (commonly known as Acrylic).



Figure 9: CAEN SP5607 Gamma absorption tool with different absorbers (Adapted from [14])

2.9 Cables and connectors

Several types of cables are available. Apart from common USB cables there are power cables, which are meant to be plugged into the devices and simply conduct electrical power. Furthermore, there are coaxial cables; this is the type of cables used to transport signals. In figure 10 the constituents of a coaxial cable can be seen.

All available coaxial cables have an impedance of 50Ω (common for signal cables in nuclear and astro-physics). This matches well with the input impedances of available instruments, which is necessary for avoiding reflections at impedance changes. In order to avoid reflections at open ends, so-called terminators are used there.

As a rule of thumb, the signal speed within coaxial cables is around $\frac{2}{3}c$, i.e. 20 cm cable length delay the signal by 1 ns.

Two types of connectors are present on the ends of the cable: LEMO-00

plugs (the larger ones) and MCX (smaller). Just use the ones matching the inputs of the respective instruments.

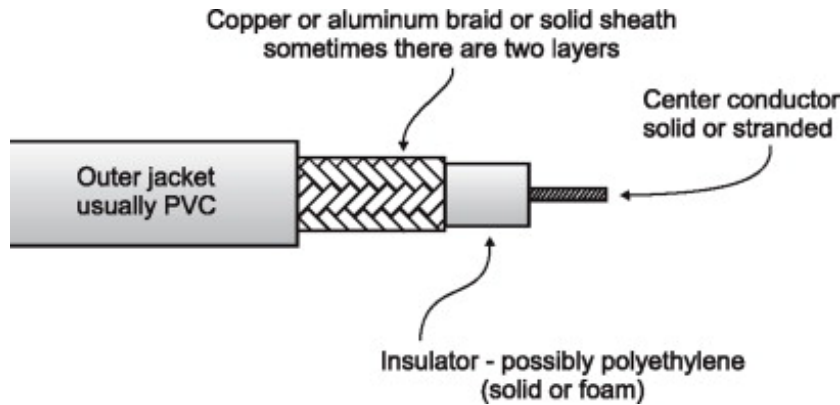


Figure 10: Typical constituents of a coaxial cable: The center conductor transporting the actual signals. The dielectric surrounds the inner conductor insulating the inner conductor and providing a certain impedance. The outer braid (usually grounded) shields the center conductor from environmental noise. The outer jacket insulating the outer braid (Adapted from [15])

2.10 Laptop and Data acquisition software

A windows computer with software to readout and control the devices is provided.

3 Measurement and Analysis

3.1 Breakdown Voltage and Gain

Determine the breakdown voltage and the Gain of the SiPM in your setup and choose from that an operation voltage. This is done by recording a energy spectrum of the SiPM at a certain voltage. The distance between two single photoelectron peaks is the gain. Plot the gain vs the bias voltage for different bias voltages to determine the breakdown voltage.

3.2 Dark Count Rate

Think about how you would measure the DCR of the SiPM with the given components. Build this setup and determine the DCR as a function of the discrimination threshold.

3.3 Cut-off threshold

Now think about how you could measure cosmic radiation with the described components. With that setup measure again the counting rate as a function of the discrimination threshold. Plot the DCR and the rate of this setup against the discrimination threshold and determine the best value for the discrimination threshold to reduce random coincidences below the Hertz level. What is the value for the cosmic rate?

3.4 System efficiency

Considering the zenith dependence of the flux ($I(\theta) = I_v \cos\theta^2$) and the integration over the solid angle, calculate the expected cosmic rate due to the system geometry and evaluate the detection efficiency.

3.5 Further tasks

Discuss your results and think about how to make the measurement setup more efficient. Also describe a possible experimental setup with which to determine the cosmic flux as a function of the zenith angle.

3.6 Report style

The write-up should have the format of a scientific work and contain all information about materials, procedures, results and analysis that a typical physics student would need to understand the results. It should contain:

1. A detailed explanation and sketch of your experimental setup(s).
2. A plot of the gain vs bias voltage with fit.
3. A plot of the DCR and the cosmic rate vs the discrimination threshold
4. Statistical uncertainties for each measured value
5. Discussion of the systematic uncertainties in each part of the experiment (which ones are there, which are the dominant ones, how could this be improved?)

Please keep in mind to cite a reference for all figures and statements that you have not created yourself. Number your references and list them at the end of the manuscript.

References

- [1] The Arecibo Observatory <http://www.naic.edu/ao>
- [2] The Very Large Telescope <https://www.eso.org/public/teles-instr/paranal-observatory/vlt>
- [3] COBE <https://science.nasa.gov/missions/cobe>
- [4] Gaisser, T., Engel, R., & Resconi, E. (2016). Cosmic Rays and Particle Physics (2nd ed.). Cambridge: Cambridge University Press.
- [5] Tanabashi M. et al. (Particle Data Group), Phys. Rev. D 98, 030001 (2018) and 2019 update.
- [6] IceCube Neutrino Observatory <https://icecube.wisc.edu>
- [7] Pacific Ocean Neutrino Explorer (P-ONE) <https://www.pacific-neutrino.org>
- [8] Borexino Collaboration <http://borex.lngs.infn.it>
- [9] CRESST Collaboration <https://www.cresst.de>
- [10] LEGEND Collaboration <http://legend-exp.org>
- [11] LIGO <https://www.ligo.caltech.edu>
- [12] The Nobel Prize in Physics 2017. Nobel Media AB 2021. <https://www.nobelprize.org/prizes/physics/2017/press-release>
- [13] SensL, An Introduction to the Silicon Photomultiplier, <https://www.sensl.com/downloads/ds/TN%20-%20Intro%20to%20SPM%20Tech.pdf>
- [14] CAEN Group, <https://www.caen.it>
- [15] J. Crisp, Introduction to Copper Cabling, 2002